Am J Cancer Res 2026;16(6):2518-2533
www.ajcr.us /ISSN:2156-6976/ajcr0172909

Original Article

IGF2BP1 orchestrates glycolytic reprogramming via HK2 to accelerate hepatocellular carcinoma malignancy

Qing Wang[1*], Hui Miao[2*], Yizhou Wang[3], Jianhong Zeng[4], Zhiping Hu[5]

[1]Department of Hepatobiliary Medicine, Eastern Hepatobiliary Surgery Hospital, The Third Affiliated Hospital of Naval Military Medical University, Naval Medical University, Shanghai 200438, China; [2]Department of Integrative Medicine, Eastern Hepatobiliary Surgery Hospital, The Third Affiliated Hospital of Naval Military Medical University, Naval Medical University, Shanghai 200438, China; [3]Department of Hepatic Surgery IV and Clinical Research Institute, Eastern Hepatobiliary Surgery Hospital, The Third Affiliated Hospital of Naval Military Medical University, Naval Medical University, Shanghai 200438, China; [4]Department of Breast, Hubei Cancer Hospital, Tongji Medical College, Huazhong University of Science and Technology, Wuhan 430079, Hubei, China; [5]Department of Integrated Traditional Chinese and Western Medicine, Hubei Cancer Hospital, Tongji Medical College, Huazhong University of Science and Technology, Wuhan 430079, Hubei, China. [*]Equal contributors and co-first authors.

Received March 27, 2026; Accepted June 10, 2026; Epub June 15, 2026; Published June 30, 2026

Abstract: Dysregulated glucose metabolism is a hallmark of hepatocellular carcinoma (HCC), yet the upstream regulators driving this metabolic reprogramming remain incompletely understood. In this study, insulin-like growth factor 2 mRNA-binding protein 1 (IGF2BP1) was identified as a critical oncogenic driver in HCC. Clinically, IGF2BP1 is markedly overexpressed in HCC tissues and cell lines, with expression levels correlating strongly with tumor aggressiveness. Functionally, silencing IGF2BP1 significantly attenuated HCC cell proliferation, migration, and invasion, concomitant with a profound suppression of glycolytic flux. Mechanistically, we demonstrate that IGF2BP1 directly binds to and stabilizes HK2 mRNA, thereby upregulating Hexokinase 2 (HK2) protein expression. This stabilization triggers a metabolic cascade characterized by increased glucose uptake, lactate production, pyruvate accumulation, and elevated lactate dehydrogenase A (LDHA) levels. Crucially, HK2 knockdown completely abrogated the pro-glycolytic and pro-tumorigenic effects induced by IGF2BP1, confirming HK2 as a critical downstream effector. In vivo xenograft models further corroborated these findings, showing that IGF2BP1 depletion drastically inhibited tumor growth while downregulating the HK2/LDHA axis and reducing pyruvate levels. Collectively, our study elucidates a novel IGF2BP1/HK2 axis that drives HCC malignancy via glycolytic reprogramming, highlighting IGF2BP1 as a promising prognostic biomarker and therapeutic target.

Keywords: Hepatocellular carcinoma, IGF2BP1, HK2, glycolysis

Introduction

Hepatocellular carcinoma (HCC), one of the most common primary liver cancers, imposes a substantial global burden in terms of incidence and mortality, especially in regions with endemic hepatitis B or C infection [1]. Although recent therapeutic advances have improved outcomes for certain patients with advanced-stage disease, the overall 5-year survival remains under 20%, largely attributable to profound tumor heterogeneity, challenges in early detection, and resistance to conventional chemotherapy [2, 3]. Therefore, an in-depth analysis of the key molecular mechanisms driving the occurrence and progression of HCC, especially the identification of central regulators of tumor metabolic reprogramming, is urgently needed.

Metabolic reprogramming is recognized as a fundamental hallmark of cancer that broadly contributes to tumor progression. Within this spectrum of metabolic dysregulation, aberrant activation of glycolysis, also known as the Warburg effect, represents a pivotal mechanism driving hepatocarcinogenesis. This metabolic adaptation allows malignant cells to meet the increased bioenergetic and biosynthetic

https://doi.org/10.62347/EZPS5229

requirements required for rapid proliferation, stress adaptation, and immune escape [4, 5]. Given that glycolysis is tightly controlled by rate-limiting enzymes, identifying which glycolytic regulators are co-opted in HCC is crucial for understanding its metabolic dependency.

Hexokinase 2 (HK2), the first rate-limiting enzyme in glycolysis, catalyzes the phosphorylation of glucose to glucose-6-phosphate and serves as a key node in regulating glycolysis flux [6]. Multiple studies have confirmed that HK2 is significantly upregulated in HCC tissues, and its expression level is closely related to tumor size, vascular invasion, TNM staging, and poor patient prognosis [7, 8]. Importantly, pharmacological inhibition or genetic knockdown of HK2 significantly inhibits HCC proliferation, migration, and in vivo tumorigenicity, suggesting that HK2 is not only a central mediator of HCC metabolic reprogramming but also a potential therapeutic target [9, 10].

Despite these findings, the upstream regulatory mechanisms underlying the aberrant overexpression of HK2 in HCC remain incompletely elucidated. In recent years, RNA binding proteins (RBPs) have attracted increasing attention in tumor biology due to their critical roles in regulating mRNA stability, translation efficiency, and intracellular localization during post-transcriptional processes. Insulin-like growth factor 2 mRNA binding protein 1 (IGF2BP1), a member of the IGF2BP family, is widely reported to be overexpressed in various malignancies, where it promotes tumor stemness, drug resistance, and metastasis by stabilizing oncogenic transcripts such as MYC mRNA [11]. For instance, in esophageal squamous cell carcinoma, IGF2BP1 binds to and stabilizes INHBA mRNA to increase INHBA protein expression, leading to activation of Smad2/3 signaling and promoting malignant phenotype [12]. In addition, IGF2BP1 is highly expressed in various HCC cell lines, suggesting its potential universal role in HCC progression [13, 14]. These studies collectively indicate the broad oncogenic functions of IGF2BP1 in HCC.

Although the individual roles of IGF2BP1 and HK2 in HCC have been well documented, their functional interplay has not been systematically investigated. Specifically, it remains unclear whether IGF2BP1 directly modulates HK2-dependent glycolytic reprogramming in HCC. In contrast, preliminary clues have been obtained in other tumor types. For example, Li et al. reported that MYO16-AS1 competitively binds to RBP IGF2BP3, thereby reducing the interaction between IGF2BP3 and HK2 mRNA, decreasing HK2 mRNA stability, inhibiting glucose metabolic reprogramming, and suppressing the invasive capacity of lung adenocarcinoma (LUAD) cells both *in vitro* and *in vivo* [15]. In HCC, Wilms tumor 1-associating protein (WTAP) has been shown to promote metabolic reprogramming by enhancing HK2 mRNA stability and consequently increasing HK2 expression [16]. These findings suggest that RBPs can regulate HK2 through post-transcriptional mechanisms, thereby affecting tumor metabolism. However, whether IGF2BP1 regulates HK2 in a similar manner, especially in the context of HCC, remains unknown.

Based on these observations, we hypothesized that IGF2BP1 promotes HCC progression by stabilizing HK2 mRNA, thereby enhancing HK2 protein expression and activating glycolytic metabolism. To test this hypothesis, we systematically investigated the role of the IGF2BP1/HK2 axis in regulating glycolytic reprogramming and HCC progression. Our findings provide new insights into the mechanisms by which IGF2BP1 promotes HCC progression and may offer a theoretical basis for the development of novel therapeutic strategies.

Materials and methods

Cell culture and clinical samples

Human hepatocellular carcinoma cell lines Huh7, HepG2, and SMMC-7721 (sourced from the American Type Culture Collection, ATCC) were cultured in DMEM containing 10% fetal bovine serum (FBS). Human normal liver LO2 cells were cultured in RPMI-1640 medium (Gibco, Thermo Fisher Scientific) containing 10% FBS (Gibco, Thermo Fisher Scientific, USA). All cells were maintained under standard conditions at 37°C in a humidified incubator containing 5% CO_2. siRNA targeting IGF2BP1 and HK2, as well as corresponding negative control siRNA (NC-siRNA), were designed and synthesized by Shanghai Jima Biotechnology Co., Ltd. (Shanghai, China). The IGF2BP1 overexpression plasmid and corresponding empty vector were purchased from Guangzhou RiboBio Co., Ltd. (Guangzhou, China). Cell transfection was

performed with Lipofectamine™ 3000 (Invitrogen, Thermo Fisher Scientific, USA) according to the manufacturer's instructions. After 6 h of transfection, medium was replaced with fresh complete culture medium, followed by an additional 48 h culture.

A total of 20 paired hepatocellular carcinoma tissues and matched adjacent non-tumorous liver specimens were harvested from patients who underwent surgical treatment at Hubei Cancer Hospital. Written informed consent was obtained from all participants before specimen collection. This study was approved by the Ethics Committee of Hubei Cancer Hospital and conducted in accordance with the Declaration of Helsinki.

Animals

Twelve 4-week-old BALB/c nude mice were purchased from Beijing Vital River Laboratory Animal Technology Co., Ltd. (Beijing, China) and acclimatized for one week under specific pathogen-free environment. After harvesting, cells were resuspended at a concentration of 1×10^7 cells/100 μL and maintained on ice. The mice were randomized into either the NC-si or IGF2BP1-si groups (n = 6). Each mouse received a subcutaneous injection of 100 μL of the corresponding cell suspension into the axillary area. Tumor dimensions (length and width) were measured every two days after inoculation, and tumor growth curves were plotted. On day 28 after inoculation, tumor tissues were harvested for subsequent analyses. All animal procedures were approved by the Animal Ethics Committee of Hubei Cancer Hospital and were conducted in accordance with institutional guidelines for animal welfare. To minimize animal suffering, mice were deeply anesthetized with pentobarbital sodium prior to euthanasia by cervical dislocation. Death was confirmed by the absence of breathing and heartbeat. Harvested tumor specimens were then either snap-frozen in liquid nitrogen or fixed in 4% paraformaldehyde for further analysis.

Western blotting

Harvested cells or tissues were rinsed thrice with PBS (Gibco, Thermo Fisher Scientific, USA) and lysed in cold RIPA buffer (Beyotime Biotechnology, Shanghai, China) supplemented with protease and phosphatase inhibitors. After centrifugation at 12,000 rpm for 5 min at 4°C, the supernatants were collected, and protein concentrations were determined using a BCA assay kit.

Prepare 10% separation gel and concentrated gel, and store at 4°C overnight after gel preparation. Equal amounts protein sample were mixed with loading buffer, denatured by boiling for 5 min, and separated by 10% sodium dodecyl sulfate-polyacrylamide gel electrophoresis (SDS-PAGE). The separated proteins were subsequently transferred onto polyvinylidene fluoride (PVDF) membranes using a wet-transfer system. After film transfer, the membranes were sealed with 5% skim milk powder in TBST for at least 1 h at room temperature and then incubated overnight at 4°C with primary antibodies against IGF2BP1 (1:1000), LDHA (1:1500), HK2 (1:800), and β-actin (1:5000). The following day, membranes were washed three times with TBST and incubated with HRP-conjugated goat anti-rabbit IgG secondary antibody (1:10000) for 1 h at room temperature. After washing, protein bands were visualized using an ECL detection kit (SuperSignal™ West Pico PLUS, Thermo Fisher Scientific). The blots were imaged using a chemiluminescence imaging system, and the intensity of the bands was semi-quantified using ImageJ (National Institutes of Health, Bethesda, MD, USA).

Reverse transcription quantitative polymerase chain reaction (RT-qPCR)

Total RNA was extracted from cultured cells using RNAiso Plus (Takara, Japan) according to the manufacturer's instructions. The isolated RNA was reverse-transcribed into complementary DNA (cDNA) using PrimeScript™ RT Master Mix (Takara, Japan). Real-time quantitative PCR was conducted using a QuantStudio™ 5 Real-Time PCR System (Thermo Fisher Scientific, Waltham, MA, USA). Each 10 μL reaction mixture consisted of 5 μL SYBR Green Premix Ex Taq™ II (Takara, Japan), 0.4 μL each of forward and reverse primers (10 μM), 1 μL cDNA template, and 3.2 μL nuclease-free water. The amplification conditions were as follows: initial denaturation at 95°C for 30 s, followed by 40 cycles of 95°C for 5 s and 60°C for 30 s. Amplification specificity was verified via melting curve analysis. Relative gene expression levels were normalized to GAPDH and quantified using the $2^{-\Delta\Delta Ct}$ method.

Immunohistochemical (IHC) assay

Tissue samples were fixed in formalin for 48 h (4°C), rinsed with distilled water, dehydrated using an automatic tissue processor, embed in paraffin, and sectioned at 4 μm thickness. Slice were mounted onto glass slides, and baked at 65°C for 40 min. Tissue sections were deparaffinized in xylene, rehydrated in graded ethanol, and rinsed with PBS. Citrate-based antigen retrieval was performed in a pressure cooker for 3 min, followed by cooling and endogenous peroxidase quenching with 3% hydrogen peroxide. Non-specific binding sites were blocked with 5% normal goat serum (30 min, room temperature). Sections were incubated with primary antibody (1:1000) overnight at 4°C, followed by a 15-min incubation at 37°C with HRP-conjugated goat anti-rabbit IgG secondary antibody (1:10000). Color development was performed using 3,3'-diaminobenzidine (DAB) for 2 min, after which the reaction was terminated with distilled water. Sections were counterstained with hematoxylin for 90 s and differentiated with 0.1% hydrochloric acid for 5 s. Slides were dehydrated through graded ethanol, cleared in xylene, and mounted. Staining was visualized and photographed under a light microscope. Staining intensity of positive cells was quantified using ImageJ software. Semi-quantitative scoring was independently performed by two pathologists blinded to the clinical data, taking both staining intensity and the proportion of positive cells into account.

CCK-8 assay

Cells were seeded in 96-well plates (100 μL/well, n = 3 per group) and allowed to adhere overnight in a Thermo Fisher Scientific incubator (USA). Subsequently, 0.1 mL of 10% CCK-8 solution (Beyotime Biotechnology, Shanghai, China) was introduced into each well at 24, 48, and 72 h without generating bubbles, and the plates were incubated for 2 h at 37°C in the dark. Absorbance at 450 nm were measured using a microplate reader (SpectraMax i3x, Molecular Devices, USA). Cell proliferation curves were generated based on the absorbance values over time.

Colony formation assay

Cells were seeded at 500 cells per well in 6-well culture plates containing complete medium and incubated under standard conditions (37°C, 5% CO_2) for two weeks until visible colonies formed. Colonies were fixed with 4% paraformaldehyde for 30 min, stained with 0.1% crystal violet for 30 min, gently washed with water and air-dried. Only colonies containing > 50 cells were counted for analysis.

Wound-healing assay

Cells were inoculated into 6-well plates and cultured until reaching approximately 90% confluence. The culture medium was discarded, and the monolayer was gently rinsed with PBS. A straight-line scratch was made across the center of each well using a sterile 200 μL pipette tip. The initial wound (0 h) was photographed under an inverted microscope. PBS was then replaced with 2 mL of serum-free medium, and incubated for an additional 48 h. Wound closure was imaged at 48 h under the microscope, and cell migration ability was evaluated by measuring the reduction in scratch width.

Transwell invasion assay

For the invasion assay, Transwell inserts were pre-coated with 30 μL Matrigel diluted in serum-free medium (1:6 ratio) to polymerize at room temperature. Cells were seeded into the upper chamber and 600 μL of complete medium containing 10% FBS was added to the lower chamber. After 24 h incubation, non-invading cells on the upper chamber were removed. Invaded cells on the underside of the membrane were fixed with methanol for 30 min and stained with 0.5% crystal violet for 30 min. After three PBS washes, stained cells were visualized and photographed under an inverted microscope. Quantification was performed by counting cells in multiple random microscopic fields.

Lactic acid production and glucose consumption

Cells were seeded and cultured under standard conditions. Culture supernatants were collected at specified time points. Extracellular lactate and glucose concentrations were measured using commercial kits (manufacturer, catalog number) according to the manufacturer's instructions. Lactate and glucose consumption were normalized to cell number or protein content to ensure comparability.

ATP content

Intracellular ATP levels were determined using the Beyotime ATP Assay Kit according to the manufacturer's protocol. Culture medium was removed, and cells were lysed by adding lysis buffer at 1/10 of the culture volume. The lysate was centrifuged, and the supernatant was collected for analysis. ATP standards of known concentrations were prepared to generate a standard curve. ATP detection reagent was mixed with diluent in a 1:9 ratio to prepare the working solution (100 μL per well/tube). Sample or standard solutions were incubated with the working solution, and relative light unit (RLU) was detected using a chemiluminescence analyzer. Intracellular ATP concentrations were calculated based on the standard curve.

Pyruvate assay

Pyruvate levels were measured using a commercial pyruvate assay kit (Beyotime Biotechnology, Shanghai, China) according to the manufacturer's instructions. Tissue samples were homogenized in lysis buffer and centrifuged to obtain the supernatant. The resulting supernatant was mixed with the assay working solution and incubated in the dark for 30 min. Optical density readings were obtained at the specified wavelength on a SpectraMax i3x reader (Molecular Devices, USA). Pyruvate levels were quantified via a standard curve and adjusted for protein concentration.

Actinomycin D assay for evaluating mRNA stability

Cells at 70-80% confluence were exposed to 5 μg/mL actinomycin D to block new mRNA synthesis, then harvested at 0, 3, 6, 9, and 12 h. After washing with PBS and extracting total RNA, RT-qPCR was performed to assess target and reference gene mRNA levels. Data were normalized relative to the 0-h time point, and the percentage of remaining mRNA was plotted against time to derive a decay curve, from which mRNA half-life was calculated to evaluate mRNA stability.

Statistical analysis

All experiments were performed in triplicate, and data were presented as mean ± standard deviation (SD). Statistical analyses were conducted using SPSS software (version 22.0; IBM SPSS, Chicago, IL, USA). Differences between paired tumor and adjacent non-tumor specimens were assessed using paired t-tests. Repeated-measures ANOVA was used to analyze longitudinal data, including cell viability and tumor volume measured at multiple time points. Comparisons among multiple groups were performed using one-way ANOVA followed by appropriate post-hoc tests. A two-sided p value < 0.05 was considered statistically significant.

Results

IGF2BP1 expression in HCC clinical samples and cell lines

Both the mRNA (**Figure 1A**) and protein (**Figure 1B**) levels of IGF2BP1 were significantly higher in HCC tissues than in paired adjacent non-tumorous tissues. Similarly, all HCC cell lines exhibited significantly higher IGF2BP1 mRNA (**Figure 1C**) and protein (**Figure 1D**) expression than the normal liver cell line LO2. IHC staining corroborated these findings, showing strong IGF2BP1 immunoreactivity in HCC tissues but weak staining in adjacent normal tissues. Semi-quantitative analysis demonstrated a significant increase in IGF2BP1 expression in tumor tissues (**Figure 1E**).

IGF2BP1 knockdown suppressed the malignant phenotype of HepG2 cells

IGF2BP1 knockdown significantly reduced both mRNA (**Figure 2A**) and protein (**Figure 2B**) levels of IGF2BP1 in HepG2 cells, indicating efficient silencing of IGF2BP1. CCK-8 assay demonstrated that IGF2BP1 depletion notably inhibited HepG2 cell proliferation (**Figure 2C**). Furthermore, knockdown of IGF2BP1 significantly weakened migration capacity (**Figure 2D**), cell invasion ability (**Figure 2E**), and clonogenic potential of HepG2 cells (**Figure 2F**), as evidenced by wound-healing assays, Transwell invasion assay, and Colony formation assay, respectively.

Knockdown of IGF2BP1 inhibited glycolysis in HepG2 cells

IGF2BP1 depletion significantly impaired glucose uptake (**Figure 3A**), lactate production (**Figure 3B**), and intracellular ATP levels (**Figure**

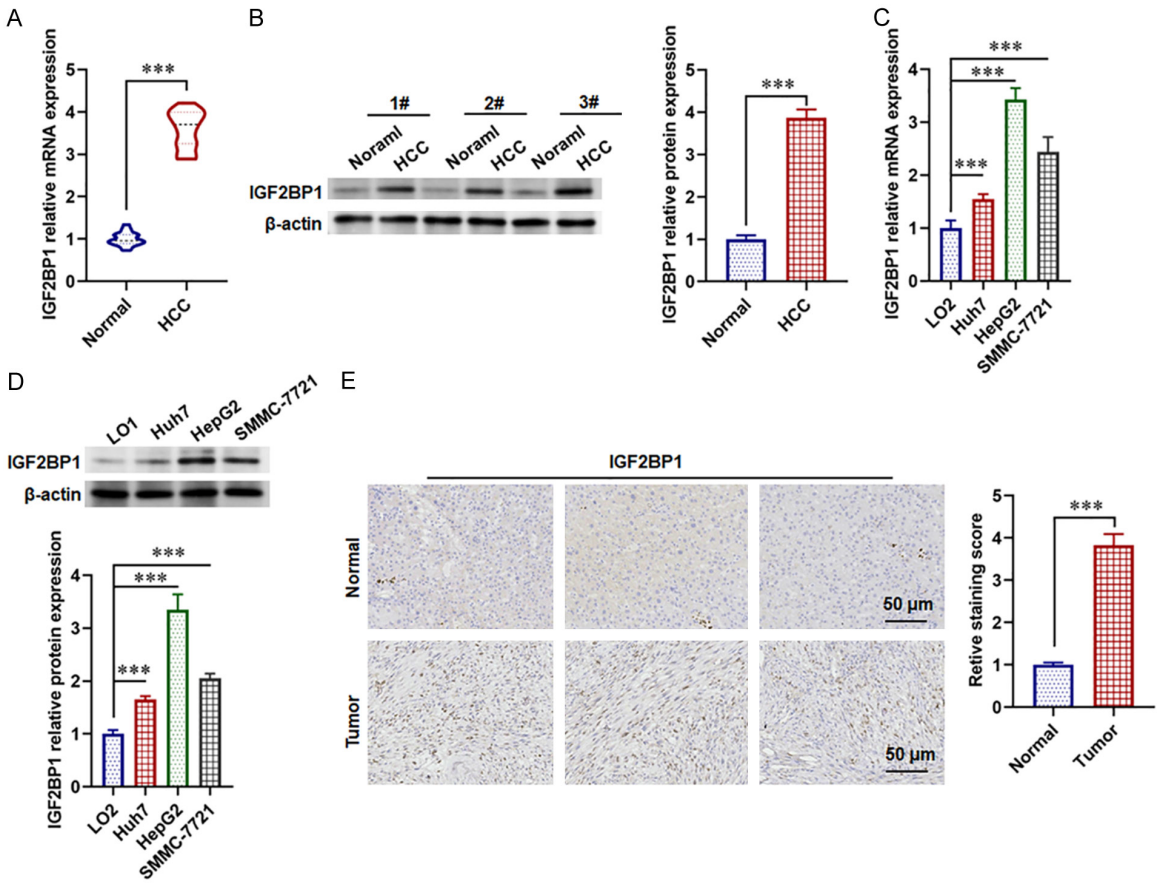

Figure 1. Expression levels of IGF2BP1 in HCC tissues and cell lines. A, B. The mRNA and protein expression levels of IGF2BP1 in HCC tissues compared with adjacent non-tumor tissues. C, D. The mRNA and protein expression levels of IGF2BP1 in the human normal liver cell line LO2 and multiple HCC cell lines (Huh7, HepG2, and SMMC-7721). E. Immunohistochemical staining of IGF2BP1 in HCC tissues with semi-quantitative analysis. Scale bar = 50 μm (200× magnification). ***P < 0.001.

3C). Consistently, intracellular pyruvate, a central glycolytic intermediate, was markedly reduced upon IGF2BP1 silencing (**Figure 3D**), accompanied by downregulation of LDHA protein expression (**Figure 3E**).

To validate these findings and explore the mechanistic role of IGF2BP1 in glycolysis, we established stable IGF2BP1-overexpressing (IGF2BP1-OE) and vector control (Vector-OE) cell lines. IGF2BP1-OE effectively elevated the mRNA (**Figure 3F**) and protein (**Figure 3G**) levels of IGF2BP1.

Functional rescue experiments were conducted in the presence of the glycolytic inhibitor 2-deoxy-D-glucose (2-DG). Under DMSO control conditions, IGF2BP1-OE significantly enhanced colony formation (**Figure 3H**) and invasive capacity (**Figure 3I**). However, 2-DG treatment attenuated the pro-proliferative and pro-invasive effects of IGF2BP1-OE, suggesting that IGF2BP1 promotes HCC cell growth and invasion at least partially through glycolytic reprogramming.

HK2 knockdown suppressed glycolysis in HepG2 cells

To elucidate the molecular mechanism by which IGF2BP1 regulates glycolysis, we focused on HK2, a key rate-limiting enzyme in the glycolytic pathway. HK2 mRNA stability was assessed using an actinomycin D chase assay. IGF2BP1 overexpression significantly prolonged the half-life of HK2 mRNA, whereas IGF2BP1 knockdown accelerated HK2 mRNA decay, confirming that IGF2BP1 stabilizes HK2 transcripts (**Figure 4A**). Furthermore, IGF2BP1 overexpression upregulated HK2 protein levels, whereas

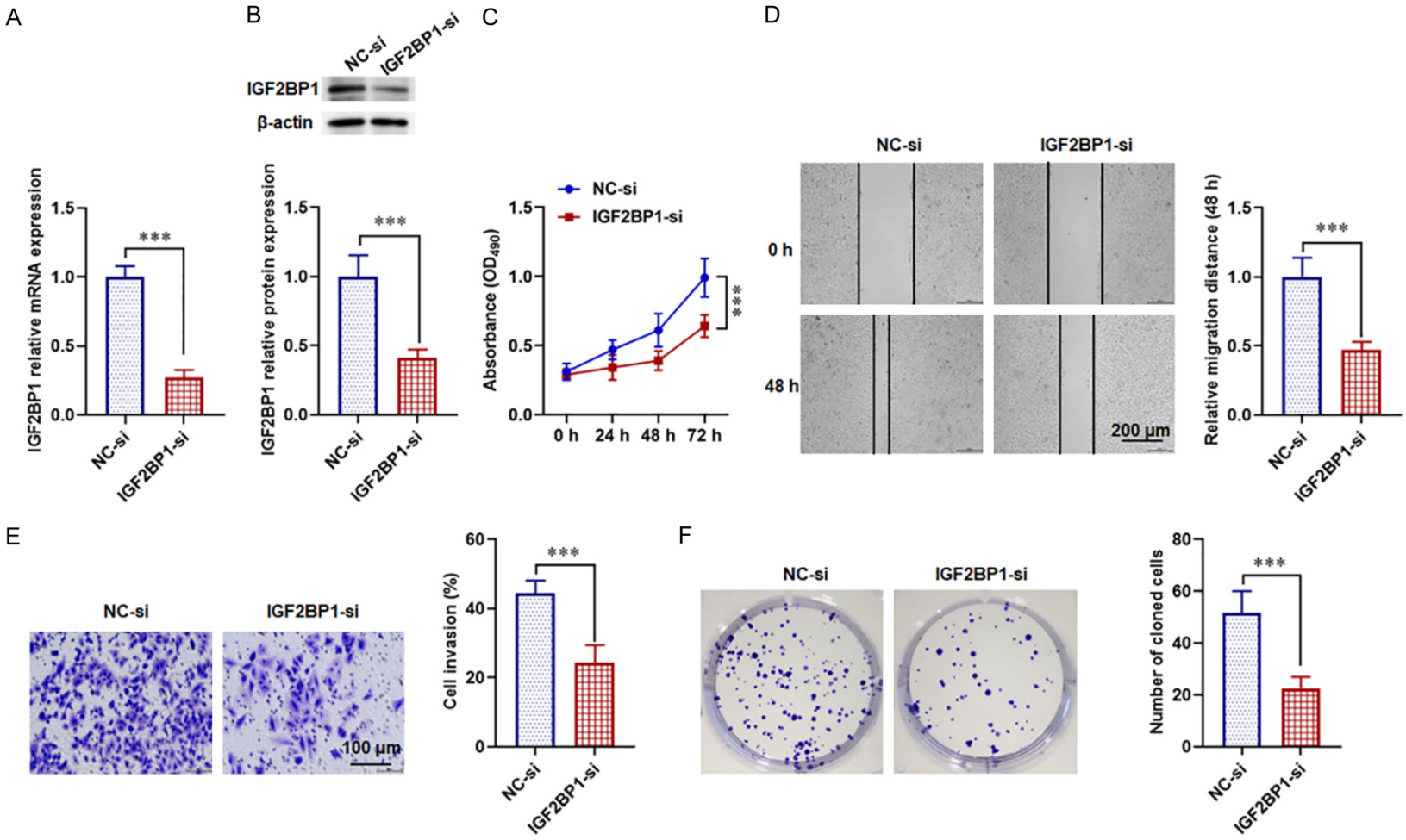

Figure 2. Effect of IGF2BP1 in the malignant phenotype of HepG2 cells. A, B Effects of IGF2BP1-si-transfection on the mRNA and protein expression levels of IGF2BP1. C. Effects of IGF2BP1-si-transfection on cell proliferation activity. D. Effects of IGF2BP1-si-transfection on cell migration at 0 h and 48 h. Scale bar = 200 μm (50× magnification). E. Effects of IGF2BP1-si-transfection on cell invasion. F. Effects of IGF2BP1-si-transfection on colony formation. Scale bar = 100 μm (100× magnification). ***P < 0.001.

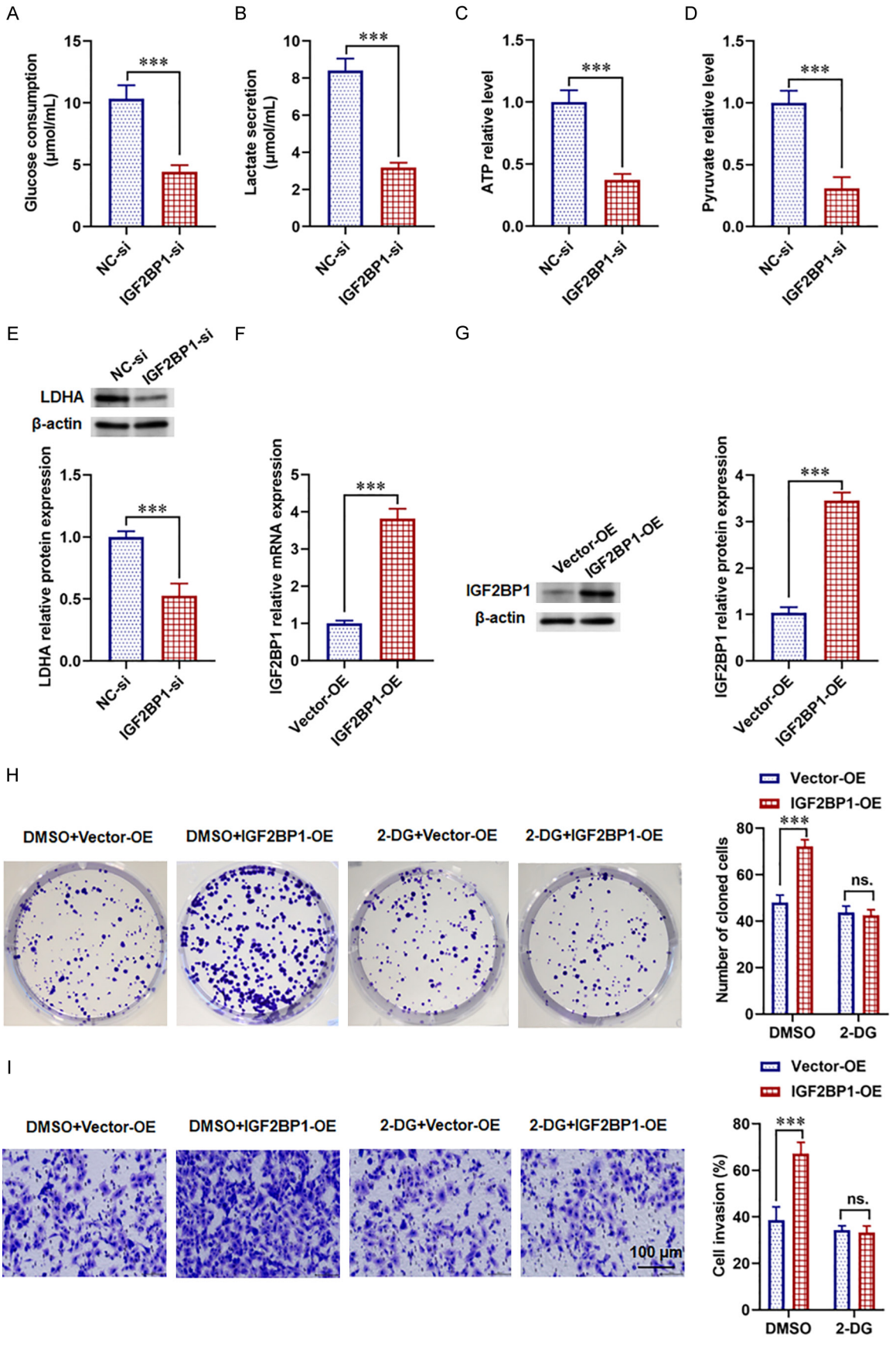
A
Glucose consumption (μmol/mL)
15
10
5
0
***
NC-si
IGF2BP1-si
B
Lactate secretion (μmol/mL)
10
8
6
4
2
0
***
NC-si
IGF2BP1-si
C
ATP relative level
1.5
1.0
0.5
0.0
***
NC-si
IGF2BP1-si
D
Pyruvate relative level
1.5
1.0
0.5
0.0
***
NC-si
IGF2BP1-si
E
NC-si
IGF2BP1-si
LDHA
β-actin
LDHA relative protein expression
1.5
1.0
0.5
0.0
***
NC-si
IGF2BP1-si
F
IGF2BP1 relative mRNA expression
5
4
3
2
1
0
***
Vector-OE
IGF2BP1-OE
G
Vector-OE
IGF2BP1-OE
IGF2BP1
β-actin
IGF2BP1 relative protein expression
4
3
2
1
0
***
Vector-OE
IGF2BP1-OE
H
DMSO+Vector-OE
DMSO+IGF2BP1-OE
2-DG+Vector-OE
2-DG+IGF2BP1-OE
Vector-OE
IGF2BP1-OE
Number of cloned cells
80
60
40
20
0
***
ns.
DMSO
2-DG
I
DMSO+Vector-OE
DMSO+IGF2BP1-OE
2-DG+Vector-OE
2-DG+IGF2BP1-OE
100 μm
Vector-OE
IGF2BP1-OE
Cell invasion (%)
80
60
40
20
0
***
ns.
DMSO
2-DG

Figure 3. Effects of IGF2BP1 on glycolysis in HepG2 cells. A. Glucose uptake levels. B. Lactate concentration in cell culture supernatant. C. ATP content. D. Pyruvate levels. E. LDHA protein expression levels. F, G. The mRNA and protein expression levels of IGF2BP1. H. Representative images and quantitative analysis of colony formation. I. Representative images and quantification of invaded cells. Scale bar = 100 μm (100× magnification). ***P < 0.001. ns: no significant difference.

IGF2BP1 knockdown reduced HK2 protein expression (**Figure 4B**), indicating that IGF2BP1 positively regulates HK2 expression at the post-transcriptional level.

We specifically silenced HK2 using siRNA to investigate the functional relevance of HK2 in HCC glycolysis. HK2-si effectively suppressed both HK2 mRNA (**Figure 4C**) and protein expression (**Figure 4D**). Moreover, HK2 knockdown significantly impaired HepG2 cell invasion (Transwell assay, **Figure 4E**) and migration (wound-healing assay, **Figure 4F**). Moreover, HK2 knockdown substantially decreased glucose uptake (**Figure 4G**), lactate production (**Figure 4H**), and pyruvate levels (**Figure 4I**), collectively indicating that HK2 is critical for maintaining glycolytic flux.

The growth inhibition induced by 2-DG was consistent with the phenotype observed upon IGF2BP1 knockdown, supporting the notion that suppression of glycolysis, particularly through HK2 downregulation, mediates anti-tumor effects. In addition, RNA immunoprecipitation experiments confirmed an interaction between IGF2BP1 and HK2 mRNA (**Figure 4J**).

In summary, IGF2BP1 promotes HK2 protein expression by stabilizing HK2 mRNA, and HK2 deficiency recapitulates the metabolic and functional phenotypes observed upon IGF2BP1 knockdown, supporting HK2 as a critical downstream effector of IGF2BP1 in glycolytic regulation.

HK2 knockdown abolished the pro-glycolytic and pro-tumorigenic effects of IGF2BP1 in HepG2 cells

To validate whether HK2 is a critical downstream effector of IGF2BP1-mediated oncogenic and glycolytic functions, rescue experiments were performed in HepG2 cells. In cells transfected with HK2-siNC, IGF2BP1 overexpression significantly increased glucose uptake (**Figure 5A**) and lactate production (**Figure 5B**). However, these effects were abolished following HK2 knockdown. Similarly, IGF2BP1 overexpression significantly increased intracellular pyruvate levels in HK2-siNC cells, whereas this increase was no longer observed in HepG2 cells with HK2 knockdown (**Figure 5C**).

Western blot analysis further revealed that IGF2BP1 overexpression upregulated LDHA protein expression in HK2-siNC cells, which was abolished after HK2 silencing (**Figure 5D**). Moreover, in the HK2-siNC group, IGF2BP1 overexpression significantly increased colony formation (**Figure 5E**) and enhanced cell invasive capacity (**Figure 5F**). In contrast, HK2 knockdown abrogated these pro-tumorigenic effects. Collectively, these findings indicate that HK2 is indispensable for IGF2BP1-mediated glycolytic activation and malignant phenotypes, supporting HK2 as a critical downstream effector of IGF2BP1 in HCC.

IGF2BP1 knockdown suppressed HCC tumor growth in vivo

HepG2 cells transfected with NC-si or IGF2BP1-si were subcutaneously injected into the right axilla of nude mice to establish an *in vivo* HCC xenograft model. On day 28 post-injection, representative tumor tissues were harvested (**Figure 6A**). IGF2BP1 silencing significantly reduced tumor weight compared with the NC-si control mice (**Figure 6B**). Tumor volume kinetics also revealed that IGF2BP1 knockdown significantly inhibited tumor growth throughout the entire experimental period (**Figure 6C**), reinforcing the oncogenic contribution of IGF2BP1.

IHC staining confirmed reduced IGF2BP1 expression in tumors derived from the IGF2BP1-si group, accompanied by a concomitant decrease in HK2 expression (**Figure 6D**). To further investigate the metabolic effects of IGF2BP1 knockdown *in vivo*, protein expression and metabolite levels were examined in xenograft tumors. Consistent with the *in vitro* findings, LDHA protein level was significantly reduced in the shIGF2BP1 group (**Figure 6E**), accompanied by reduced pyruvate levels (**Figure 6F**).

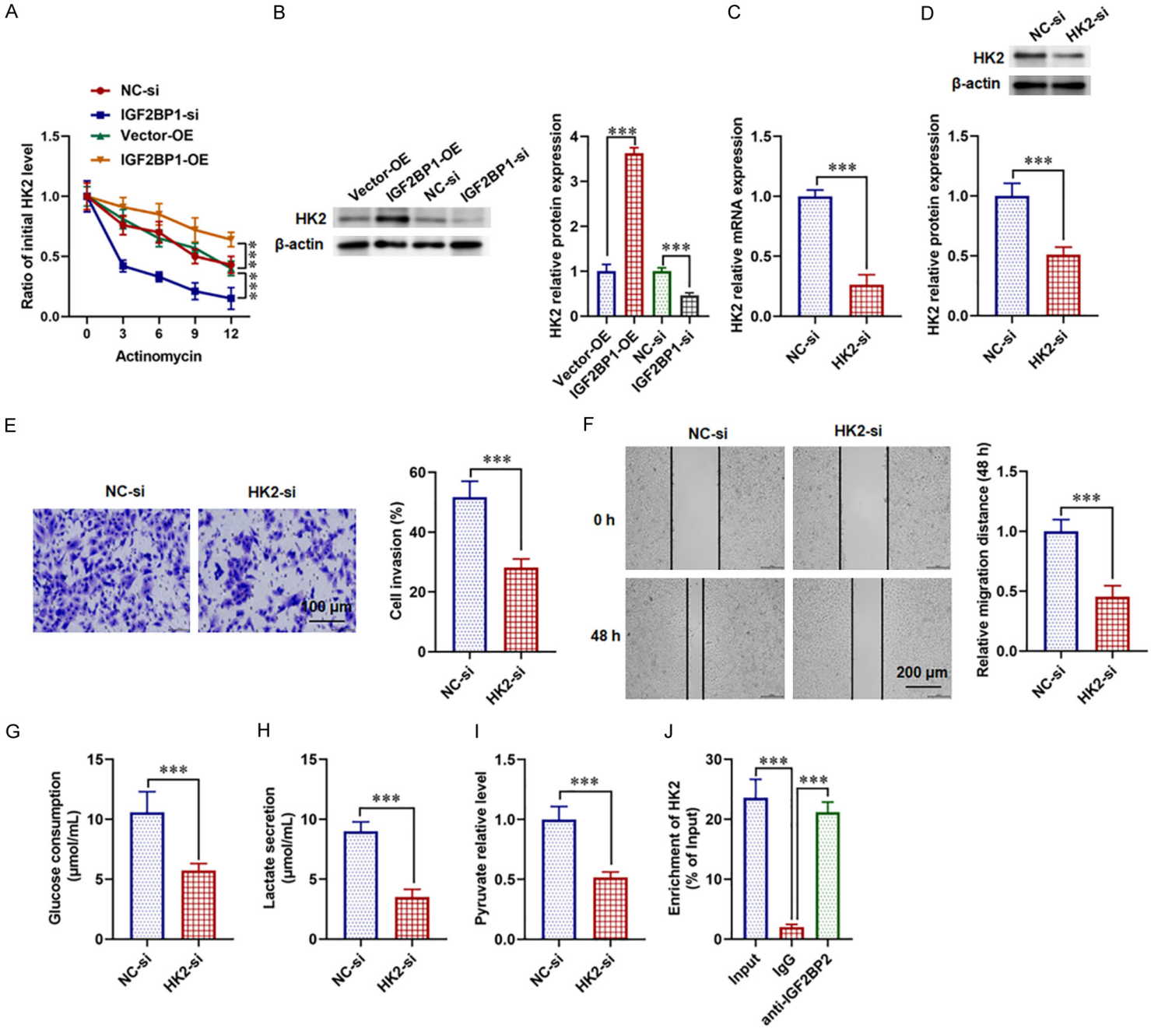
A
NC-si
IGF2BP1-si
Vector-OE
IGF2BP1-OE
Ratio of initial HK2 level
Actinomycin
B
Vector-OE
IGF2BP1-OE
NC-si
IGF2BP1-si
HK2
β-actin
HK2 relative protein expression
C
HK2 relative mRNA expression
D
NC-si
HK2-si
HK2
β-actin
HK2 relative protein expression
E
NC-si
HK2-si
100 μm
Cell invasion (%)
F
NC-si
HK2-si
0 h
48 h
200 μm
Relative migration distance (48 h)
G
Glucose consumption (μmol/mL)
H
Lactate secretion (μmol/mL)
I
Pyruvate relative level
J
Enrichment of HK2 (% of Input)
Input
IgG
anti-IGF2BP2

Figure 4. The role of HK2 in glycolysis in HepG2 cells. A. Actinomycin D assay assessing HK2 mRNA stability. B. HK2 protein expression levels. C. HK2 mRNA levels. D. HK2 protein expression levels. E. Representative images and quantification of Transwell invasion assay. Scale bar = 100 μm (100× magnification). F. Wound healing assay at 0 h and 48 h. Scale bar = 200 μm (50× magnification). G. Glucose uptake. H. Lactate production. I. Pyruvate levels. J. RNA immunoprecipitation experiments were conducted to demonstrate the physical binding between IGF2BP1 and HK2 mRNA. ***P < 0.001.

Discussion

This study systematically elucidates the molecular mechanism by which RBP IGF2BP1 promotes HCC cell proliferation, invasion, and *in vivo* tumor growth by upregulating HK2 expression and activating the glycolysis pathway. Our data not only demonstrate upregulation of IGF2BP1 in HCC clinical samples and cell lines, but also highlight that its oncogenic function is largely mediated through HK2-dependent glycolysis reprogramming. The identification of the "IGF2BP1-HK2 glycolysis" axis provides a new functional perspective for understanding the HCC metabolic dependency and underscores a broader role of RBP in regulating tumor energy metabolism.

Clinical sample analysis showed that both mRNA and protein levels of IGF2BP1 were significantly higher in HCC tissues than those in adjacent tissues. IHC analysis further demonstrated that high IGF2BP1 expression is associated with adverse pathological features. These observations are highly consistent with multiple independent studies. For example, elevated IGF2BP1 expression has been associated with increased tumor volume, vascular invasion, and reduced overall survival [17]. Similar phenomena have been reported in gastric cancer and colorectal cancer, indicating that IGF2BP1 can enhance tumor stemness and metastatic potential [18, 19]. Although our cohort primarily assessed differential expression, accumulating evidence from large-scale clinical studies supports the prognostic significance of IGF2BP1. Notably, interrogation of The Cancer Genome Atlas (TCGA) data indicates that IGF2BP1 overexpression correlates with advanced TNM stage and poor overall survival in diverse malignancies, including colorectal cancer [20]. Mechanistically, functional studies in gastric cancer demonstrated that IGF2BP family proteins can stabilize HK2 mRNA via m6A modification to promote glycolysis, promoting glycolysis and tumor progression [21]. Consistently, our *in vitro* experiments showed that IGF2BP1 knockdown significantly inhibited HCC cell proliferation, colony formation, migration, and invasion, supporting its role as a key driving factor for HCC progression.

IGF2BP1 deficiency significantly suppressed multiple glycolytic parameters in HCC cells, including glucose uptake, lactate production, and pyruvate accumulation, and ATP generation, accompanied by reduced expression of the glycolytic enzyme LDHA. These findings indicate that IGF2BP1 functions as an important regulator of HCC glycolysis reprogramming. Furthermore, treatment of IGF2BP1-overexpressing cells with the glycolysis inhibitor 2-DG significantly weakened the promotive effects of IGF2BP1 on cell proliferation and invasion, indicating that enhanced glycolysis activity is required for IGF2BP1 to exert its tumor-promoting effects. These observations are consistent with studies demonstrating that HK2 deficiency induces metabolic stress and impairs tumor growth in vivo, while normal tissues exhibit relatively high tolerance to HK2 deficiency [22, 23]. Collectively, these findings support that targeting glycolytic metabolism may represent a selective anti-tumor strategy for HCC.

More importantly, our study identified that IGF2BP1 promotes HK2 protein expression by stabilizing HK2 mRNA, and knocking down HK2 alone can suppress the glycolytic activity and malignant phenotype induced by IGF2BP1 deficiency. The carcinogenic role of HK2, as the first rate-limiting enzyme in glycolysis, has been widely confirmed in HCC. HK2 is frequently overexpressed in HCC tissues, and elevated HK2 expression has been significantly correlated with poor prognosis [24]. Other studies have shown that pharmacological or genetic inhibition of HK2 can enhance the anti-tumor efficacy of sorafenib, highlighting its potential as a therapeutic target in HCC treatment [25, 26]. Despite the recognized importance of HK2 in tumor metabolism, the upstream mechanisms governing its dysregulation, especially the post-transcriptional regulation, remain incompletely understood. Accumulating evidence suggests that IGF2BP2 recognizes the m^6A site

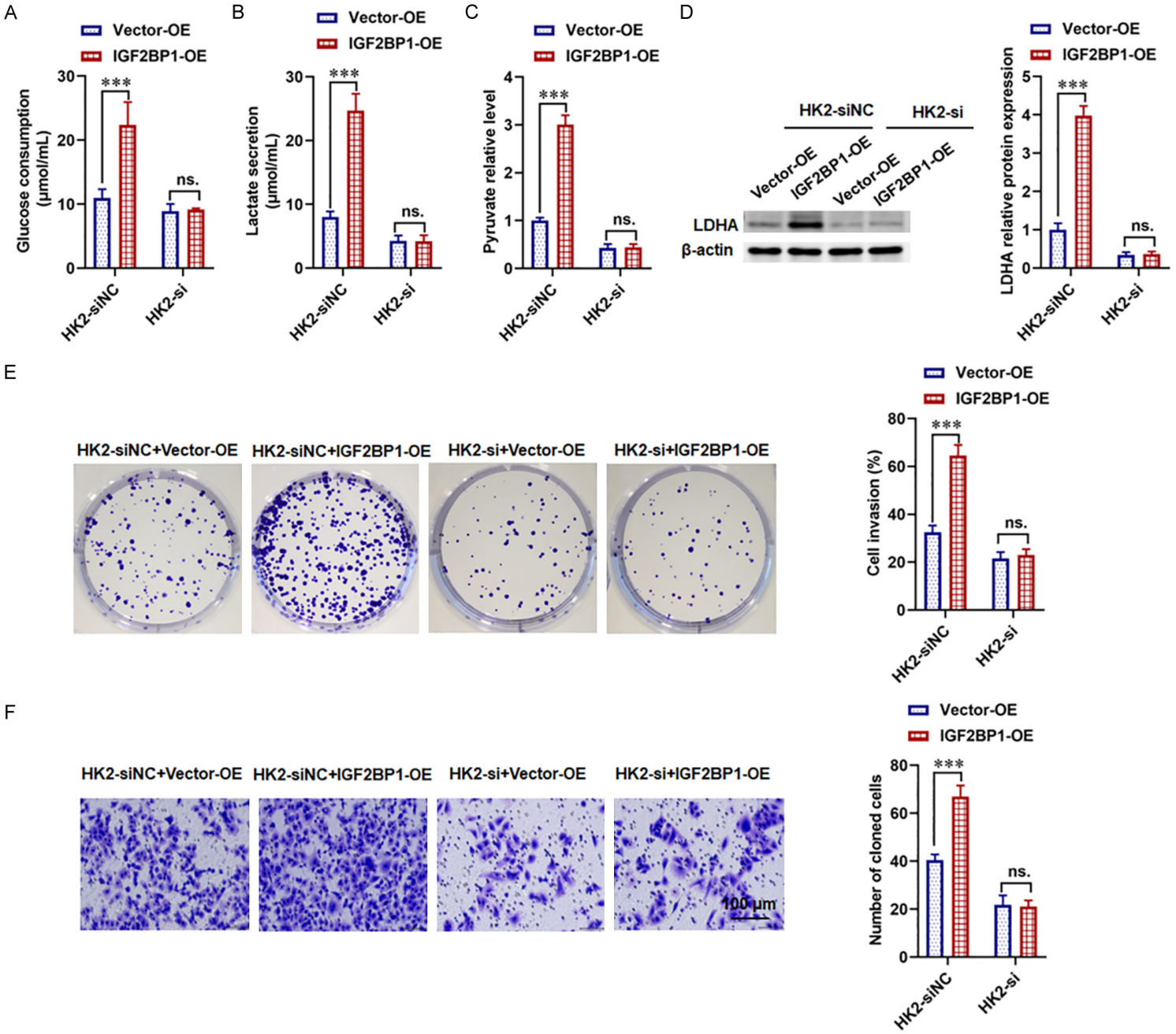
A
Vector-OE
IGF2BP1-OE
Glucose consumption (μmol/mL)
***
ns.
HK2-siNC
HK2-si
B
Lactate secretion (μmol/mL)
C
Pyruvate relative level
D
HK2-siNC
HK2-si
LDHA
β-actin
LDHA relative protein expression
E
HK2-siNC+Vector-OE
HK2-siNC+IGF2BP1-OE
HK2-si+Vector-OE
HK2-si+IGF2BP1-OE
Cell invasion (%)
F
Number of cloned cells
100 μm

Figure 5. The role of HK2 in IGF2BP1-mediated tumorigenesis and glycolysis promotion. A. Glucose uptake levels. B. Lactate concentration. C. Pyruvate levels. D. LDHA protein expression levels. E. Representative images and quantitative analysis of colony formation. F. Representative images and quantification of invaded cells. Scale bar = 100 μm (100× magnification). ***P < 0.001. ns: no significant difference.

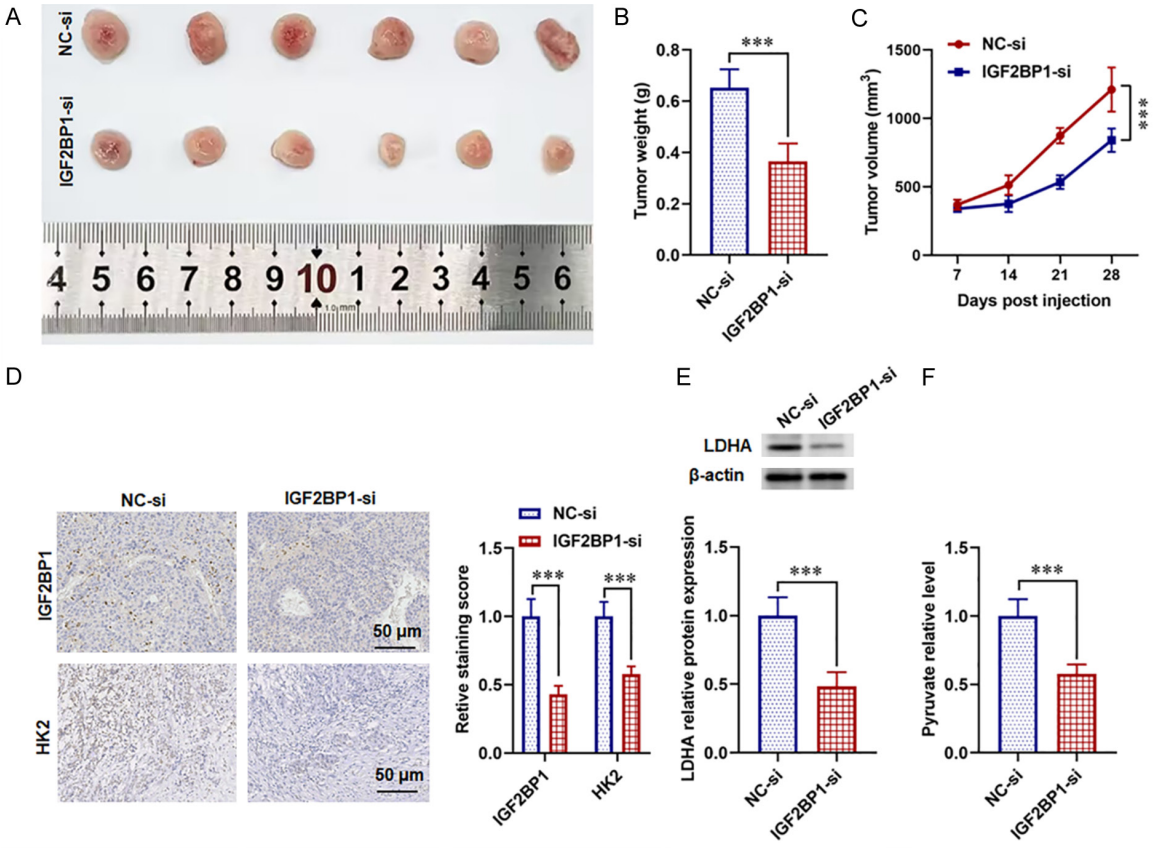

Figure 6. IGF2BP1 promotes tumorigenicity in vivo. A. Representative images of tumor tissues. B. Tumor tissue weights. C. Tumor volume growth curves. D. Immunohistochemical staining and quantitative analysis of IGF2BP1 and HK2 expression in tumor tissues. E. Western blotting images and quantification of LDHA protein levels. F. Pyruvate content in tumor tissues. Scale bar = 50 μm (200× magnification). ***P < 0.001.

of CASC9 to form the IGF2BP2/CASC9 complex, which enhances the stability of HK2 mRNA and promotes aerobic glycolysis in glioblastoma [27].

Our study incorporated IGF2BP1 into the regulatory network governing HK2 expression, indicating that IGF2BP1 enhances glycolytic flux by stabilizing HK2 mRNA or enhancing its translation efficiency. Although this study did not delve into specific binding sites or modes of action, the rescue experiments provide compelling functional evidence supporting this regulatory relationship. Specifically, HK2 knockdown abolished the ability of IGF2BP1 overexpression to enhance glycolytic activity and promote invasive ability, indicating that HK2 is a downstream effector mediating IGF2BP1's oncogenic function. In addition, we confirmed in a nude mouse subcutaneous xenograft model that knocking down IGF2BP1 significantly inhibits tumor growth, accompanied by reduced LDHA protein expression and decreased intratumoral pyruvate content. IHC analysis further demonstrated concomitant downregulation of IGF2BP1 and HK2 in xenograft tumors, supporting their functional association during HCC progression. Our in vivo findings bridge the gap between molecular regulation and metabolic phenotype. The accumulation of pyruvate serves as a direct readout of glycolytic inhibition, strongly supporting the notion that IGF2BP1 depletion

disrupts energy metabolism in the tumor. This metabolic disruption, characterized by impaired LDHA function and blocked glycolytic flux, is likely a primary driver of the observed tumor growth suppression. These observations are highly consistent with previous studies demonstrating HK2 overexpression drives tumor growth, and also confirm the central role of sustained glycolytic activity in tumor maintenance in vivo [28, 29]. While 2-DG is a pan-inhibitor of hexokinases rather than a specific HK2 inhibitor, our findings strongly support HK2 as a principal downstream effector mediating IGF2BP1-driven tumor progression. This is based on the following observations: First, HK2 serves as the rate-limiting enzyme in glycolysis and is frequently elevated in HCC. Second, IGF2BP1 directly regulates HK2 expression by enhancing HK2 mRNA stability. Third, the phenotypic effects induced by IGF2BP1 overexpression were largely abolished following HK2 knockdown. These findings collectively indicate that activation of the IGF2BP1-HK2 axis represents a major mechanism through which IGF2BP1 promotes glycolytic reprogramming and malignant progression in HCC.

Despite these findings, several limitations should be acknowledged. First, although our metabolomic data revealed pyruvate accumulation upon IGF2BP1 knockdown, supporting a functional link between IGF2BP1 and glycolytic regulation, we were unable to perform a direct genetic rescue experiment by re-expressing HK2 in IGF2BP1-deficient cells. Therefore, while our data strongly implicate HK2 as a critical downstream node, we cannot completely exclude the contribution of other IGF2BP1-regulated metabolic targets. Future studies employing HK2 overexpression or catalytic mutant rescue approaches will be necessary to conclusively establish HK2 as the necessary and sufficient effector of IGF2BP1-mediated metabolic reprogramming. Second, all mechanistic investigations were conducted exclusively in HepG2 cells. Although HepG2 is a well-characterized HCC model, it may not fully represent the molecular heterogeneity of clinical HCC, particularly HBV-associated subtypes. Therefore, the generalizability of our findings to other HCC etiologies and subtypes warrants further validation using additional cell line models and patient-derived samples in future studies.

Conclusion

IGF2BP1 plays a key regulatory role in glycolytic reprogramming in HCC. IGF2BP1 directly binds to HK2 mRNA, enhances its stability, and upregulates HK2 expression, thereby promoting glycolytic activity and malignant progression. Disruption of the IGF2BP1-HK2 axis suppresses glycolytic metabolism and tumor growth. These findings not only deepens our understanding of the oncogenic mechanism of IGF2BP1, but also provides a theoretical basis for the development of novel therapeutic strategies targeting the IGF2BP1-HK2 signaling axis in HCC treatment.

Disclosure of conflict of interest

None.

Address correspondence to: Jianhong Zeng, Department of Breast, Hubei Cancer Hospital, Tongji Medical College, Huazhong University of Science and Technology, No 116 Zhuodaoquan South Road, Hongshan District, Wuhan 430079, Hubei, China. E-mail: 1226242401@qq.com; Zhiping Hu, Department of Integrated Traditional Chinese and Western Medicine, Hubei Cancer Hospital, Tongji Medical College, Huazhong University of Science and Technology, No 116 Zhuodaoquan South Road, Hongshan District, Wuhan 430079, Hubei, China. E-mail: Zjj420106@163.com

References

[1] Ganesan P and Kulik LM. Hepatocellular carcinoma: new developments. Clin Liver Dis 2023; 27: 85-102.
[2] Konyn P, Ahmed A and Kim D. Current epidemiology in hepatocellular carcinoma. Expert Rev Gastroenterol Hepatol 2021; 15: 1295-1307.
[3] Long J, Cui K, Wang D, Qin S and Li Z. Burden of hepatocellular carcinoma and its underlying etiologies in China, 1990-2021: findings from the global burden of disease study 2021. Cancer Control 2024; 31: 10732748241310573.
[4] Feng J, Li J, Wu L, Yu Q, Ji J, Wu J, Dai W and Guo C. Emerging roles and the regulation of aerobic glycolysis in hepatocellular carcinoma. J Exp Clin Cancer Res 2020; 39: 126.
[5] Zhang Y, Li W, Bian Y, Li Y and Cong L. Multifaceted roles of aerobic glycolysis and oxidative phosphorylation in hepatocellular carcinoma. PeerJ 2023; 11: e14797.
[6] Zheng Y, Zhan Y, Zhang Y, Zhang Y, Liu Y, Xie Y, Sun Y, Qian J, Ding Y, Ding Y and Fang Y. Hexo-

kinase 2 confers radio-resistance in hepatocellular carcinoma by promoting autophagy-dependent degradation of AIMP2. Cell Death Dis 2023; 14: 488.
[7] Cheng M, Wang B, Duan L, Jin Y, Zhang W and Li N. HOTAIR knockdown increases the sensitivity of hepatocellular carcinoma cells to sorafenib by disrupting miR-145-5p/HK2 axis-mediated mitochondrial function and glycolysis. Front Biosci (Landmark Ed) 2025; 30: 37368.
[8] Zhao L, Kang M, Liu X, Wang Z, Wang Y, Chen H, Liu W, Liu S, Li B, Li C, Chang A and Tang B. UBR7 inhibits HCC tumorigenesis by targeting Keap1/Nrf2/Bach1/HK2 and glycolysis. J Exp Clin Cancer Res 2022; 41: 330.
[9] Mai RY, Ye JZ, Gao X, Wen T, Li SZ, Zeng C, Cen WJ, Wu GB, Lin Y, Liang R and Luo XL. Up-regulated ITGB4 promotes hepatocellular carcinoma metastasis by activating hypoxia-mediated glycolysis and cancer-associated fibroblasts. Eur J Pharmacol 2025; 986: 177102.
[10] Ye J, Xiao X, Han Y, Fan D, Zhu Y and Yang L. MiR-3662 suppresses cell growth, invasion and glucose metabolism by targeting HK2 in hepatocellular carcinoma cells. Neoplasma 2020; 67: 773-781.
[11] Yang F, Xue X, Zheng L, Bi J, Zhou Y, Zhi K, Gu Y and Fang G. Long non-coding RNA GHET1 promotes gastric carcinoma cell proliferation by increasing c-Myc mRNA stability. FEBS J 2014; 281: 802-13.
[12] Wang JJ, Chen DX, Zhang Y, Xu X, Cai Y, Wei WQ, Hao JJ and Wang MR. Elevated expression of the RNA-binding protein IGF2BP1 enhances the mRNA stability of INHBA to promote the invasion and migration of esophageal squamous cancer cells. Exp Hematol Oncol 2023; 12: 75.
[13] Li QZ, Chen YY, Liu QP, Feng ZH, Zhang L and Zhang H. Cucurbitacin B suppresses hepatocellular carcinoma progression through inducing DNA damage-dependent cell cycle arrest. Phytomedicine 2024; 126: 155177.
[14] Guo C, Zhou N, Lu Y, Mu M, Li Z, Zhang X, Tu L, Du J, Li X, Huang D, Xu Q and Zheng X. FGF19/FGFR4 signaling contributes to hepatocellular carcinoma survival and immune escape by regulating IGF2BP1-mediated expression of PD-L1. Biomed Pharmacother 2024; 170: 115955.
[15] Li P, Ge H, Zhao J, Zhou Y, Zhou J, Li P, Luo J, Zhang W, Tian Z and Zhao X. Disrupting of IGF2BP3-stabilized HK2 mRNA by MYO16-AS1 competitively binding impairs LUAD migration and invasion. Mol Cell Biochem 2024; 479: 2795-2808.
[16] Niu Y, Jia S, Xiao X, Tu K and Liu Q. High glucose facilitates hepatocellular carcinoma cell proliferation and invasion via WTAP-mediated HK2 mRNA stability. Mol Cell Biochem 2025; 480: 4149-4168.
[17] Lixin S, Wei S, Haibin S, Qingfu L and Tiemin P. miR-885-5p inhibits proliferation and metastasis by targeting IGF2BP1 and GALNT3 in human intrahepatic cholangiocarcinoma. Mol Carcinog 2020; 59: 1371-1381.
[18] Jiang T, Xia Y, Li Y, Lu C, Lin J, Shen Y, Lv J, Xie L, Gu C, Xu Z and Wang L. TRIM29 promotes antitumor immunity through enhancing IGF2BP1 ubiquitination and subsequent PD-L1 downregulation in gastric cancer. Cancer Lett 2024; 581: 216510.
[19] Singh V, Walter V, Elcheva I, Imamura Kawasawa Y and Spiegelman VS. Global role of IGF-2BP1 in controlling the expression of Wnt/β-catenin-regulated genes in colorectal cancer cells. Front Cell Dev Biol 2023; 11: 1236356.
[20] Meng Q, Xiang H, Wang Y, Hu K, Luo X, Wang J, Chen E, Zhang W, Chen J, Chen X, Wang H, Ju Z and Song Z. Exosomes containing circSCP2 in colorectal cancer promote metastasis via sponging miR-92a-1-5p and interacting with PTBP1 to stabilize IGF2BP1. Biol Direct 2024; 19: 130.
[21] Shen C, Xuan B, Yan T, Ma Y, Xu P, Tian X, Zhang X, Cao Y, Ma D, Zhu X, Zhang Y, Fang JY, Chen H and Hong J. m(6)A-dependent glycolysis enhances colorectal cancer progression. Mol Cancer 2020; 19: 72.
[22] Li WC, Huang CH, Hsieh YT, Chen TY, Cheng LH, Chen CY, Liu CJ, Chen HM, Huang CL, Lo JF and Chang KW. Regulatory role of hexokinase 2 in modulating head and neck tumorigenesis. Front Oncol 2020; 10: 176.
[23] Wang H, Wang L, Zhang Y, Wang J, Deng Y and Lin D. Inhibition of glycolytic enzyme hexokinase II (HK2) suppresses lung tumor growth. Cancer Cell Int 2016; 16: 9.
[24] Meng YM, Jiang X, Zhao X, Meng Q, Wu S, Chen Y, Kong X, Qiu X, Su L, Huang C, Wang M, Liu C and Wong PP. Hexokinase 2-driven glycolysis in pericytes activates their contractility leading to tumor blood vessel abnormalities. Nat Commun 2021; 12: 6011.
[25] Wei Q, Ren Y, Zheng X, Yang S, Lu T, Ji H, Hua H and Shan K. Ginsenoside Rg3 and sorafenib combination therapy relieves the hepatocellular carcinomaprogression through regulating the HK2-mediated glycolysis and PI3K/Akt signaling pathway. Bioengineered 2022; 13: 13919-13928.
[26] Yu Q, Dai W, Ji J, Wu L, Feng J, Li J, Zheng Y, Li Y, Cheng Z, Zhang J, Wu J, Xu X and Guo C. Sodium butyrate inhibits aerobic glycolysis of hepatocellular carcinoma cells via the c-myc/hexokinase 2 pathway. J Cell Mol Med 2022; 26: 3031-3045.

[27] Liu H, Qin S, Liu C, Jiang L, Li C, Yang J, Zhang S, Yan Z, Liu X, Yang J and Sun X. m(6)A reader IGF2BP2-stabilized CASC9 accelerates glioblastoma aerobic glycolysis by enhancing HK2 mRNA stability. Cell Death Discov 2021; 7: 292.

[28] Zhang N, Zhang H, Yang X, Xue Q, Wang Q, Chang R, Zhu L, Chen Z and Liu X. USP14 exhibits high expression levels in hepatocellular carcinoma and plays a crucial role in promoting the growth of liver cancer cells through the HK2/AKT/P62 axis. BMC Cancer 2024; 24: 237.

[29] Zeng Z, Xu S, Wang R and Han X. FKBP4 promotes glycolysis and hepatocellular carcinoma progression via p53/HK2 axis. Sci Rep 2024; 14: 26893.